ACS APPLIED MATERIALS & INTERFACES

Research Article

www.acsami.org

In Situ Synthesis of Graphene Molecules on TiO_2: Application in Sensitized Solar Cells

Zhiqiang Ji,[†] Ruilian Wu,[‡] Lyudmyla Adamska,[§] Kirill A. Velizhanin,[§] Stephen K. Doorn,[∥] and Milan Sykora*,[†]

[†]Chemistry Division, [‡]Bioscience Division, [§]Theory Division, Center for Nonlinear Studies, [∥]Materials Physics and Applications Division, Center for Integrated Nanotechnologies, Los Alamos National Laboratory, Los Alamos, New Mexico 87545, United States

Supporting Information

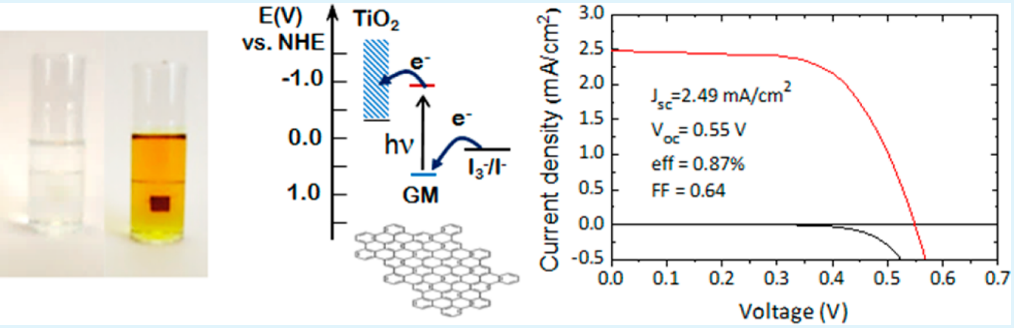

ABSTRACT: We present a method for preparation of graphene molecules (GMs), whereby a polyphenylene precursor functionalized with surface anchoring groups, preadsorbed on surface of TiO_2, is oxidatively dehydrogenated in situ via a Scholl reaction. The reaction, performed at ambient conditions, yields surface adsorbed GMs structurally and electronically equivalent to those synthesized in solution. The new synthetic approach reduces the challenges associated with the tendency of GMs to aggregate and provides a convenient path for integration of GMs into optoelectronic applications. The surface synthesized GMs can be effectively reduced or oxidized via an interfacial charge transfer and can also function as sensitizers for metal oxides in light harvesting applications. Sensitized solar cells (SSCs) prepared from mesoscopic TiO_2/GM films and an iodide-based liquid electrolyte show photocurrents of ~2.5 mA/cm^2, an open circuit voltage of ~0.55 V and fill factor of ~0.65 under AM 1.5 illumination. The observed power conversion efficiency of η = 0.87% is the highest reported efficiency for the GM sensitized solar cell. The performance of the devices was reproducible and stable for a period of at least 3 weeks. We also report first external and internal quantum efficiency measurements for GM SSCs, which point to possible paths for further performance improvements.

KEYWORDS: *graphene molecule, nanographene, graphene quantum dot, Scholl reaction, sensitized solar cell*

INTRODUCTION

Small graphene structures called graphene molecules (GMs) or graphene quantum dots have been recently attracting a growing interest because of their appealing optical and electronic properties.[1−5] Theory predicts that these graphene fragments, a few nanometers in size, are subject to quantum confinement effects similar to those observed in inorganic semiconductor quantum dots, but with different scaling laws, excited state properties and effects of functionalization.[6−9] Predictions of unique size-dependent properties of GMs suggest the possibility that their experimental studies will lead to the observation of interesting new phenomena and potentially development of new technologies. However, systematic experimental studies of the electronic structure and demonstration of applications have so far been limited, in part due to challenges associated with the preparation of well-defined structures.

GMs can be prepared by a number of methods typically categorized into "top-down" and "bottom-up" approaches. In the top-down approach, GMs are prepared by chemical or physical cleaving of exfoliated graphene or graphene-oxide sheets. Large quantities of GMs with good solubility in polar solvents can be efficiently prepared by these methods. However, significant dispersion in size and chemical functionalization of the resulting structures makes the studies of their electronic properties and integration into applications challenging. In the bottom-up approach, the GMs are prepared in a multistep chemical synthesis from simple molecular precursors, yielding uniform ensembles of GMs. A versatile synthetic methodology for the preparation of GMs and larger polycyclic aromatic hydrocarbons in excellent yields, based on intra-

Received: September 5, 2014
Accepted: October 16, 2014
Published: October 16, 2014

dx.doi.org/10.1021/am506047f | ACS Appl. Mater. Interfaces 2014, 6, 20473−20478

molecular oxidative dehydrogenation,[10] was developed by Müllen and co-workers.[2,11−13] In spite of high control over structural properties of synthesized GMs, their characterization and effective device integration can be challenging due to the tendency of GMs to aggregate via π-stacking interactions, resulting in low solubility in common solvents. Recently, GM solubilization strategies based on peripheral functionalization of GMs with bulky[14−16] or polar[17] functional groups were demonstrated, facilitating systematic studies of optical properties of synthesized GMs.[15,18,19] In cases when the functionalization limits the ability of GMs to participate in charge transfer processes,[20] this strategy may not be effectively utilized in practical applications.

The abundance of the key constituent, carbon, the high photochemical stability and the tunability of the electronic properties make GMs very attractive materials for application in photovoltaics.[21−24] Tunability of their bandgap to the near-infrared range (NIR)[16,25] makes GMs appealing chromophores for sensitized solar cells (SSCs), where they could help address limited solar spectrum coverage of commonly used sensitizers/dyes. The tendency of GMs to aggregate, however, makes their effective integration into SSC devices difficult. Li and co-workers demonstrated that the GMs solubilized by peripheral functionalization with long aliphatic chains can sensitize TiO_2 and produce photocurrent in SSCs.[20] However, even in this case effective integration of the GMs into the devices was challenging and the performance of the devices was low.

Herein we report a new approach to preparation of GMs based on in situ oxidation of a precursor preadsorbed on the surface of TiO_2. The new synthetic approach reduces the challenges associated with the tendency of GMs to aggregate without extensive peripheral functionalization, while providing a convenient path for preparation of composite materials suitable for development of optoelectronic applications. We demonstrate that the new approach can be used to improve performance of GM SSCs.

■ EXPERIMENTAL SECTION

The new synthetic approach is summarized in Scheme 1. In a first step, a polyphenylene precursor (P1) functionalized with one or more carboxylic acid functional groups is prepared by methods described previously (see the Supporting Information for more details).[12,15] Exposure of nanocrystalline TiO_2 film to a dichloromethane solution of P1 (conc. 0.1 mM, 15 h.) at room temperature led to adsorption of P1 onto the film, as confirmed by Fourier transform infrared (FTIR) spectroscopy (see below). After the film is washed with dichloromethane, the TiO_2/P1 film is exposed at RT to an argon saturated solution of $FeCl_3$ (10 mg/mL) in CH_3NO_2/CH_2Cl_2 (1:3 v/v). Within seconds, the film became colored, indicating conjugation of aromatic rings of the surface adsorbed P1. This is consistent with previous reports of effective oxidation of polyphenylene precursors functionalized with carboxylic acids or esters in solution.[18] After 1 h under the above reaction conditions, the film is washed with dichloromethane and methanol and air-dried. The resulting color of the dry film is dark red, which we attribute to the formation of GMs on the TiO_2 surface.

Scheme 1. Abbreviated Summary of the Procedure for the in Situ Synthesis of GMs on TiO_2[a]

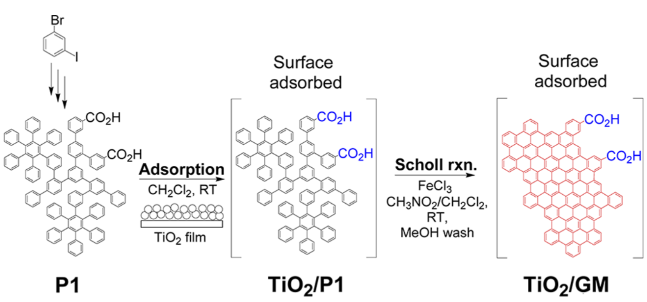

[a]Detailed synthetic procedure for P1 preparation is shown in the Supporting Information, Figure S1.

■ RESULTS AND DISCUSSION

As discussed in more detail elsewhere,[3] the large size and rigidity of GMs and their tendency to aggregate makes traditional ensemble methods, such as elemental analysis, or NMR ineffective in their characterization, even when prepared in solution.[26] So far, matrix-assisted laser desorption/ionization (MALDI)-mass spectroscopy and IR vibrational spectroscopy are the most commonly used methods for structural characterization of GMs and larger polycyclic aromatic hydrocarbons (PAHs). We have adapted these methods for characterization of surface synthesized GMs and performed additional characterization by absorption spectroscopy and electrochemistry as summarized below.

Figure 1 shows the UV/vis absorption spectra of a TiO_2/P1 film before and after the Scholl reaction. The formation of a conjugated aromatic system is evidenced by the development of a broad absorption band with a peak at ∼470 nm, and a distinct shoulder at ∼580 nm. By naked eye, this is observed as a change in the appearance of the film from colorless to dark red (photographs in Figure 1). No color change was observed for bare TiO_2 films exposed to Scholl reaction conditions or for TiO_2/P1 films treated with only solvent. The absorption properties of the product are similar to GMs of similar structure prepared previously in solution.[15] We found that the shapes of the absorption spectra of the TiO_2/GM films were identical when the concentrations of the P1 solutions used in the preparation of the precursor TiO_2/P1 films were less than 7 μM. Small spectral broadening and a blue shift of the high energy peak was observed at higher P1 concentrations. We found that the rate of changes in absorption of the TiO_2/P1

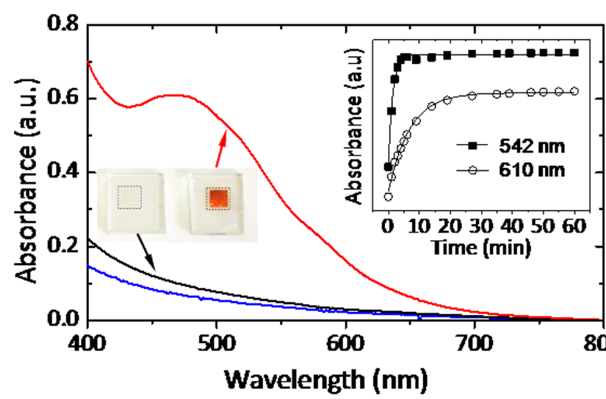

Figure 1. Electronic absorption spectra of bare TiO_2 film (blue curve), TiO_2/P1 film (black curve) and the same film after Scholl reaction (red curve). All spectra were recorded for dry films on glass substrates. The photographs show the TiO_2/P1 film before and after the Scholl reaction. The dashed lines show the location of film on the substrate. Inset: Changes in the absorption of the film with time at 542 and 610 nm observed during the exposure of the TiO_2/P1 film to the $FeCl_3$ solution (symbols). The solid lines are best fits of the expression for single exponential growth to the experimental data.

film observed following its exposure to the $FeCl_3$ solution is wavelength dependent (inset of Figure 1), reflecting the complexity of the chemical reaction. In all performed reactions, the absorption changes were 99% complete in less than 30 min.

To determine the extent of conjugation of the GM formed on the TiO_2 surface, the films were studied by diffuse reflectance FTIR spectroscopy. The representative spectra of a TiO_2/P1 and TiO_2/GM films as well as the spectra of the blank TiO_2 film, in the spectral regions ~2800−3200 and ~3900−4200 cm^{-1}, are presented in Figure 2. In the lower energy region, the spectra of the TiO_2/P1 films are dominated by a distinct multiplet of bands in the range ~3030−3100 cm^{-1}. This range is characteristic of −C−H stretching vibrations of unconjugated benzene rings, which are abundant in P1. The bands are absent in the spectrum of the TiO_2/GM, indicating a high degree of ring fusion in the product. Additional evidence indicating efficient ring fusion is available in the high energy spectral range, ~3900−4200 cm^{-1}. The presence/absence of a combination peak in this region at ~4050 cm^{-1}, associated with freely rotating benzene rings, was previously used as a signature of the presence/absence of noncondensed benzene rings in aromatic molecules.[27] In our studies, we detected a distinct peak at 4054 cm^{-1} in the spectra of TiO_2/P1.[28] This peak is completely absent in the spectra of the TiO_2/GM films, indicating absence of freely rotating rings in GMs. In addition to these features, we detected a series of three weak bands in the range ~2900−3000 cm^{-1}, for some of the films, apparent also in data shown in Figure 2. This region is characteristic of −C−H stretching vibrations of aliphatic hydrocarbons. Since these features were most dominant in the spectra of the blank TiO_2 film we assign them to surface contaminants adsorbed onto the TiO_2 film from air. The peak intensities are significantly reduced in the spectra of both TiO_2/P1 and TiO_2/GM films, which we attribute to the displacement of the contaminants from the surface during P1 adsorption and oxidation. While the inherent heterogeneities of the films resulted in variations in the recorded spectra from film-to-film and from site-to-site within a single film, the observations summarized above were consistent across all measurements. More detailed theoretical analysis of the vibrational modes of P1 and the GMs is summarized in the Supporting Information.

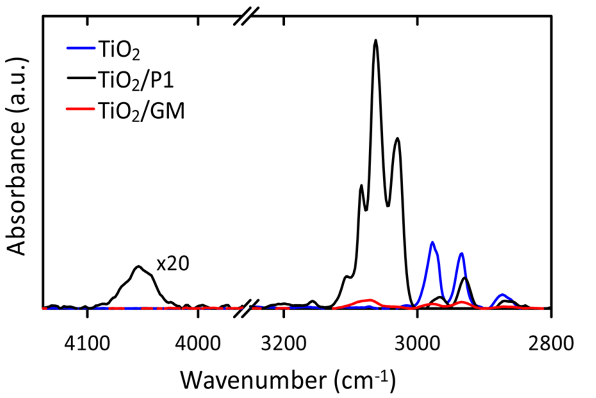

Figure 2. Diffuse reflectance FTIR spectra of dry TiO_2/P1 film in air before (black curve) and after (red curve) Scholl reaction. Also shown is the FTIR spectrum of the dry TiO_2 film before exposure to P1 (blue curve). All films were prepared on FTO substrates. In all measurements, the reflectance spectrum of FTO was used as a background. The experimental spectral resolution was 4 cm^{-1}.

To further investigate the chemical structure of the surface synthesized GMs, the structures were studied by MALDI-TOF (time-of flight) mass spectroscopy (MS). The challenges associated with MS studies of large PAHs prepared in solution, mostly related to their inefficient ionization, were previously described by Mullen et al.[29] These challenges are further amplified in the case of surface synthesized GMs. The initial efforts to study GMs ionized directly from the nanocrystalline TiO_2 surface yielded low quality signals (see the Supporting Information, Figure S15). To achieve better signal quality, a new sample preparation method was devised, whereby the GMs are chemically desorbed from the TiO_2 support prior to the MS analysis. We found that GMs can be effectively desorbed from TiO_2/GM nanoparticles when stirred in a mixture of HF/HCl (0.5 M/0.5 M) aqueous solution for 2 days. The desorbed GMs were collected by centrifugation and washed extensively with deionized (DI) water. For the MS study, the isolated GMs were mixed with a supporting matrix, TCNQ (tetracyanoquinodimethane). The MS of the GM sample prepared in this manner is shown in Figure 3a. Figure 3b shows the MS spectrum of the GM synthesized independently in solution (see the Supporting Information for details). In both cases, a dominant peak is observed at m/z of 1622 (Note: although less pronounced, a similar peak was also observed in MS studies of GM/TiO_2 films by direct desorption, see the Supporting Information, Figure S15). This peak is attributed to a species with the molecular formula $C_{132}H_{37}^{+}$. This corresponds to the fully conjugated GM structure shown on the right side of Scheme 1 (chemical formula $C_{132}H_{36}(COOH)_2$), without the carboxylic acid functional groups. The decarboxylation is most likely a result of high laser energy required for ionization of the sample.

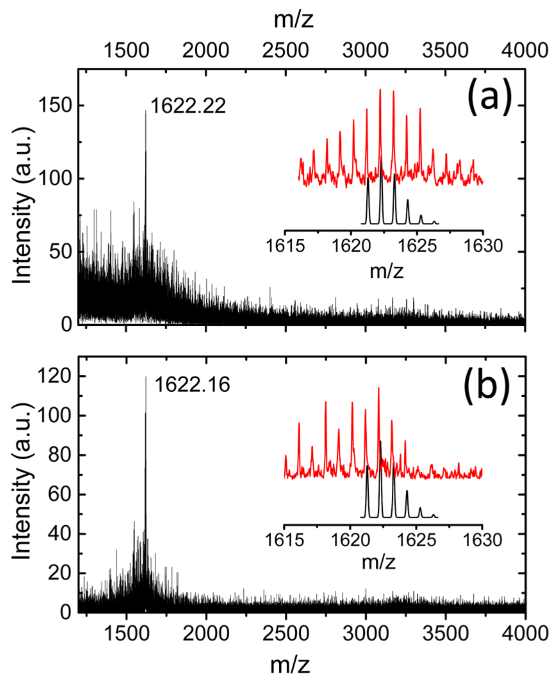

Figure 3. MALDI-TOF mass spectra of GMs synthesized on TiO_2 surface, (a) after desorption from TiO_2 surface by a dilute HF/HCl and the same GMs independently synthesized in solution (b). The molecular weight of the highest intensity mass peak is indicated. The laser energy used in the experiment was 13 μJ. Insets: the experimental (red curves) and calculated (black) isotope distribution for mass peak of $C_{132}H_{37}^{+}$.

Several small peaks observed at m/z region below 1621 are attributed to the molecular fragments of the GM generated during ionization via loss of one or more peripheral protons.

A more detailed analysis of the MS signals in the region around the main peak, shown in the insets of Figures 3a,b, reveals small deviations of the experimental isotope distribution pattern from the pattern calculated for the $C_{132}H_{37}^{+}$. The extra peaks observed in the experimental data on the low end of the m/z range are attributed to the ionization fragments of the main product $C_{132}H_{37}^{+}$. A small deviation of the intensities on the high m/z end for the surface synthesized GMs (panel a) are close to the detection limit and could be an experimental artifact. The deviation could also indicate presence of small amounts of byproducts, e.g., structures where one or more C−C bonds did not form during the Scholl reaction. However, because contamination with such byproducts is expected to translate into a population of free rotating phenyl rings, not detected in our FTIR studies discussed above, we conclude that such contamination, if present, is minor.

On the basis of the results summarized above, we conclude that the in situ surface synthesis procedure described here can be used for efficient chemical conversion of TiO_2/P1 to TiO_2/GM, where GM has the chemical composition $C_{132}H_{36}(COOH)_2$. We find that this method can be used without modifications for preparation of GMs with other chemical compositions. While the surface-mediated synthesis of nanographene structures on metals, under ultrahigh vacuum conditions, was reported previously,[30,31] to our knowledge, this is the first example of the GM surface synthesis performed under ambient conditions. We found that, in addition to TiO_2, the surface Scholl process described above is also efficient on other metal oxide surfaces such as ZrO_2 and ITO (results to be published elsewhere), indicating the generality of the method described here.

In addition to UV/vis spectroscopy, the electronic properties of the GMs were also studied by cyclic voltammetry (Supporting Information, Figure S14). In acetonitrile solution, the TiO_2/GM films show a reversible peak at ∼0.7 V (vs NHE), which we attribute to a one electron oxidation of the surface adsorbed GMs. Because TiO_2 is an insulator in this potential range, the observed oxidation of GMs only occurs near the FTO electrode. The oxidation potential observed here is very close to the ionization potential values observed for similar GMs prepared in solution by Li and co-workers.[18] Using the electrochemistry result as an approximate value for the energy of the GM HOMO, and the absorption spectrum onset (∼1.7 eV) as an approximate value for the GM band gap, we estimate the LUMO energy offset to be approximately −1.0 V (vs NHE). A comparison of these values with the known values of the energy offset of the TiO_2 conduction band and oxidation potential of the electrolyte (Figure 4a inset),[32] suggests that the GM* → TiO_2 electron injection as well as GM^{+} → electrolyte hole transfer are thermodynamically favorable. This conclusion is confirmed by the results of our device studies discussed below.

In the construction of the GM SSC, the in situ prepared TiO_2/GM film (thickness ∼7 μm) was first washed with an HCl/MeOH solution overnight to remove any adsorbed Fe species, and then rinsed with MeOH and air-dried. The removal of Fe was confirmed by X-ray photoelectron spectroscopy. The film was coupled, using a spacer, to a platinum counter electrode and complemented with a redox iodide electrolyte (Dysol, EL-HPE). Figure 4a shows an

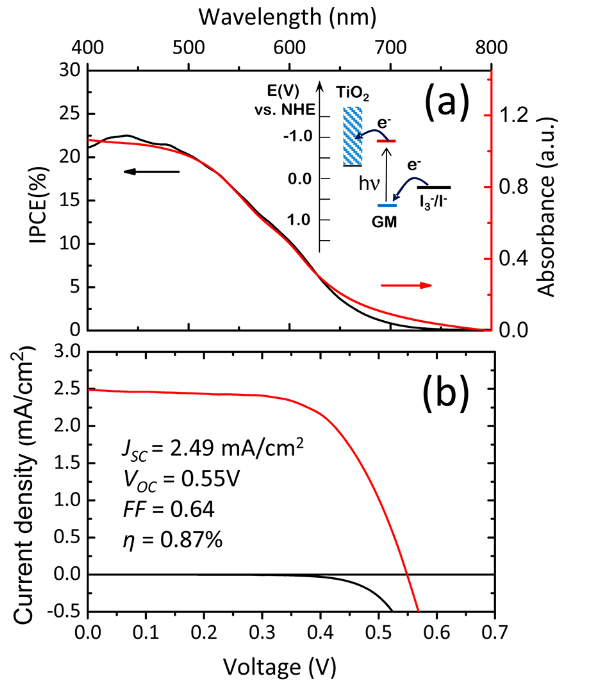

Figure 4. (a) IPCE spectrum (black curve) of the FTO/TiO_2/GM/electrolyte/Pt/FTO device and electronic absorption (red curve) of the FTO/TiO_2/GM electrode. Inset: Schematic energy diagram of the device. (b) J−V curves of the GM device in dark (black curve) and under simulated 1 sun, AM 1.5 illumination (red curve).

incident photon-to-current conversion efficiency (IPCE) spectrum of a typical GM device overlaid with the absorption spectrum of the corresponding TiO_2/GM film. The IPCE curve matches closely the absorption spectrum of the film, indicating that the photocurrent was generated via the photoexcitation of GMs. Figure 4b shows a J−V response and the performance parameters of a GM SSC that showed the best performance. To the best of our knowledge the power conversion efficiency of 0.87% is the highest reported efficiency for a sensitized solar cell using GM as a light harvesting component. The improvement compared to previous reports is attributed to the advantages of the in situ GM synthesis approach described above. We found the performance of the devices prepared by the above-described method to be very reproducible with the device-to-device variations in J_{SC}, V_{OC}, FF and η of less than 10%. In addition, we found that the devices show no degradation in performance for a period of at least 3 weeks (Supporting Information, Figure S17).

In a direct comparison study of the GM SSCs with the N3 (*cis*-Bis(isothiocyanato) bis(2,2′-bipyridyl-4,4′-dicarboxylato ruthenium(II)) dye SSCs prepared under the same conditions, we found that the efficiencies of the first-generation GM SSCs were lower by a factor of ∼5. To better understand the source of this difference, we performed measurements of internal quantum efficiencies (IQEs) for multiple devices (see the Supporting Information). We found that for the GM SSCs the IQEs were in the range of ∼20−30% (Supporting Information, Figure S16), which is significantly lower than the values of ∼100% typically observed for dye SSCs. Because the IQE is a product of charge injection and collection efficiencies, our results suggest that the overall efficiency losses are, at least in part, related to the inefficient charge transfer at the TiO_2/GM and GM/electrolyte interfaces. Detailed understanding of the charge transfer processes at these interfaces and identification of approaches for improving the device efficiencies are the subject of our future studies.

CONCLUSIONS

In summary, we have shown that polyphenylene compounds adsorbed on the surface of a nanocrystalline TiO_2 film can be successfully oxidized to GMs via the Scholl reaction. The resulting TiO_2/GM films can be used to construct functional and stable SSCs. The method described here opens a new path for direct incorporation of GMs into photoactive structures and devices.

ASSOCIATED CONTENT

Supporting Information

Experimental methods, synthetic procedures, modeling of vibrational spectra, and characterization results. This material is available free of charge via the Internet at http://pubs.acs.org.

AUTHOR INFORMATION

Corresponding Author

*M. Sykora. E-mail: sykoram@lanl.gov.

Notes

The authors declare no competing financial interest.

ACKNOWLEDGMENTS

Z.J., R.W., L.A., K.A.V., S.K.D and M.S. acknowledge the financial support by the Los Alamos National Laboratory Directed Research and Development (LDRD) program. This work was performed in part at the Center for Integrated Nanotechnologies, a U.S. Department of Energy, Office of Basic Energy Sciences user facility.

REFERENCES

(1) Muellen, K. Evolution of Graphene Molecules: Structural and Functional Complexity as Driving Forces Behind Nanoscience. *ACS Nano* **2014**, *8*, 6531−6541.

(2) Chen, L.; Hernandez, Y.; Feng, X.; Müllen, K. From Nanographene and Graphene Nanoribbons to Graphene Sheets: Chemical Synthesis. *Angew. Chem., Int. Ed.* **2012**, *51*, 7640−7654.

(3) Yan, X.; Li, B.; Li, L.-s. Colloidal Graphene Quantum Dots with Well-Defined Structures. *Acc. Chem. Res.* **2012**, *46*, 2254−2262.

(4) Li, L.; Wu, G.; Yang, G.; Peng, J.; Zhao, J.; Zhu, J.-J. Focusing on Luminescent Graphene Quantum Dots: Current Status and Future Perspectives. *Nanoscale* **2013**, *5*, 4015−4039.

(5) Bacon, M.; Bradley, S. J.; Nann, T. Graphene Quantum Dots. *Part. Part. Syst. Charact.* **2013**, *31*, 415−428.

(6) Schumacher, S. Photophysics of Graphene Quantum Dots: Insights from Electronic Structure Calculations. *Phys. Rev. B* **2011**, *83*, 081417-1−081417-4.

(7) Mandal, B.; Sarkar, S.; Sarkar, P. Exploring the Electronic Structure of Graphene Quantum Dots. *J. Nanopart. Res.* **2012**, *14*, 1−8.

(8) Ozfidan, I.; Korkusinski, M.; Guclu, A. D.; McGuire, J. A.; Hawrylak, P. Microscopic Theory of the Optical Properties of Colloidal Graphene Quantum Dots. *Phys. Rev. B* **2014**, *89*, 085310-1−085310-9.

(9) Li, L.-s.; Yan, X. Colloidal Graphene Quantum Dots. *J. Phys. Chem. Lett.* **2010**, *1*, 2572−2576.

(10) Scholl, R.; Seer, C. The Secession of Aromatic Bounded Hydrogenn and the Attachment of Aromatic Nuclei through Aluminium Chloride. *J. Liebigs Ann. Chem.* **1912**, *394*, 111−177.

(11) Watson, M. D.; Fechtenkotter, A.; Müllen, K. Big Is Beautiful - "Aromaticity" Revisited from the Viewpoint of Macromolecular and Supramolecular Benzene Chemistry. *Chem. Rev.* **2001**, *101*, 1267−1300.

(12) Simpson, C. D.; Brand, J. D.; Berresheim, A. J.; Przybilla, L.; Rader, H. J.; Mullen, K. Synthesis of a Giant 222 Carbon Graphite Sheet. *Chem.—Eur. J.* **2002**, *8*, 1424−1429.

(13) Feng, X.; Pisula, W.; Müllen, K. Large Polycyclic Aromatic Hydrocarbons: Synthesis and Discotic Organization. *Pure Appl. Chem.* **2009**, *81*, 2203−2224.

(14) Debije, M. G.; Piris, J.; de Haas, M. P.; Warman, J. M.; Tomovic, Z.; Simpson, C. D.; Watson, M. D.; Mullen, K. The Optical and Charge Transport Properties of Discotic Materials with Large Aromatic Hydrocarbon Cores. *J. Am. Chem. Soc.* **2004**, *126*, 4641−4645.

(15) Yan, X.; Cui, X.; Li, L.-s. Synthesis of Large, Stable Colloidal Graphene Quantum Dots with Tunable Size. *J. Am. Chem. Soc.* **2010**, *132*, 5944−5945.

(16) Narita, A.; Feng, X.; Hernandez, Y.; Jensen, S. A.; Bonn, M.; Yang, H.; Verzhbitskiy, I. A.; Casiraghi, C.; Hansen, M. R.; Koch, A. H. R.; Fytas, G.; Ivasenko, O.; Li, B.; Mali, K. S.; Balandina, T.; Mahesh, S.; De Feyter, S.; Muellen, K. Synthesis of Structurally Well-Defined and Liquid-Phase-Processable Graphene Nanoribbons. *Nat. Chem.* **2014**, *6*, 126−132.

(17) Tan, Y.-Z.; Yang, B.; Parvez, K.; Narita, A.; Osella, S.; Beljonne, D.; Feng, X.; Müllen, K. Atomically Precise Edge Chlorination of Nanographenes and Its Application in Graphene Nanoribbons. *Nat. Commun.* **2013**, *4*, 1−7.

(18) Yan, X.; Li, B.; Cui, X.; Wei, Q.; Tajima, K.; Li, L.-s. Independent Tuning of the Band Gap and Redox Potential of Graphene Quantum Dots. *J. Phys. Chem. Lett.* **2011**, *2*, 1119−1124.

(19) Mueller, M. L.; Yan, X.; McGuire, J. A.; Li, L.-s. Triplet States and Electronic Relaxation in Photoexcited Graphene Quantum Dots. *Nano Lett.* **2010**, *10*, 2679−2682.

(20) Yan, X.; Cui, X.; Li, B.; Li, L.-s. Large, Solution-Processable Graphene Quantum Dots as Light Absorbers for Photovoltaics. *Nano Lett.* **2010**, *10*, 1869−1873.

(21) Kang, S. J.; Ahn, S.; Kim, J. B.; Schenck, C.; Hiszpanski, A. M.; Oh, S.; Schiros, T.; Loo, Y.-L.; Nuckolls, C. Using Self-Organization to Control Morphology in Molecular Photovoltaics. *J. Am. Chem. Soc.* **2013**, *135*, 2207−2212.

(22) Xiao, S.; Kang, S. J.; Wu, Y.; Ahn, S.; Kim, J. B.; Loo, Y.-L.; Siegrist, T.; Steigerwald, M. L.; Li, H.; Nuckolls, C. Supersized Contorted Aromatics. *Chem. Sci.* **2013**, *4*, 2018−2023.

(23) Mirtchev, P.; Henderson, E. J.; Soheilnia, N.; Yip, C. M.; Ozin, G. A. Solution Phase Synthesis of Carbon Quantum Dots as Sensitizers for Nanocrystalline TiO_2 Solar Cells. *J. Mater. Chem.* **2012**, *22*, 1265−1269.

(24) Narayanan, R.; Deepa, M.; Srivastava, A. K. Forster Resonance Energy Transfer and Carbon Dots Enhance Light Harvesting in a Solid-State Quantum Dot Solar Cell. *J. Mater. Chem. A* **2013**, *1*, 3907−3918.

(25) Schwab, M. G.; Narita, A.; Hernandez, Y.; Balandina, T.; Mali, K. S.; De Feyter, S.; Feng, X.; Müllen, K. Structurally Defined Graphene Nanoribbons with High Lateral Extension. *J. Am. Chem. Soc.* **2012**, *134*, 18169−18172.

(26) To date, the largest PAH characterized by ^{1}H NMR, performed under special conditions, comprised 78 carbon carbon atoms. Schwab, M. G.; Narita, A.; Hernandez, Y.; Balandina, T.; Mali, K. S.; De Feyter, S.; Feng, X.; Mullen, K. *J. Am. Chem. Soc.* **2012**, *134*, 18169.

(27) Wu, J.; Gherghel, L.; Watson, M. D.; Li, J.; Wang, Z.; Simpson, C. D.; Kolb, U.; Müllen, K. From Branched Polyphenylenes to Graphite Ribbons. *Macromolecules* **2003**, *36*, 7082−7089.

(28) This peak was also detected in the spectra of solid P1.

(29) Przybilla, L.; Brand, J.-D.; Yoshimura, K.; Räder, H. J.; Müllen, K. MALDI-TOF Mass Spectrometry of Insoluble Giant Polycyclic Aromatic Hydrocarbons by a New Method of Sample Preparation. *Anal. Chem.* **2000**, *72*, 4591−4597.

(30) Bjork, J.; Stafstrom, S.; Hanke, F. Zipping Up: Cooperativity Drives the Synthesis of Graphene Nanoribbons. *J. Am. Chem. Soc.* **2011**, *133*, 14884−14887.

(31) Cai, J.; Ruffieux, P.; Jaafar, R.; Bieri, M.; Braun, T.; Blankenburg, S.; Muoth, M.; Seitsonen, A. P.; Saleh, M.; Feng, X.; Muellen, K.;

Fasel, R. Atomically Precise Bottom-up Fabrication of Graphene Nanoribbons. *Nature* **2010**, *466*, 470−473.
(32) Boschloo, G.; Hagfeldt, A. Characteristics of the Iodide/Triiodide Redox Mediator in Dye-Sensitized Solar Cells. *Acc. Chem. Res.* **2009**, *42*, 1819−1826.